Bulletin of the Seismological Society of America. Vol. 67, No. 2, pp. 247–258. April 1977

ACOUSTIC EMISSION AND CREEP IN ROCK AT HIGH CONFINING PRESSURE AND DIFFERENTIAL STRESS

By D. Lockner and J. Byerlee

ABSTRACT

Two samples each of Weber Sandstone and Westerly Granite were tested under triaxial compression at 1 kb confining pressure. Axial load was increased in steps, and the acoustic emission generated in the samples during primary creep was monitored. The rate ν of acoustic emission events was found to decrease exponentially at each stress level, obeying the law $\log \nu = \beta - \alpha N$, where N is the total number of microseismic events that have occurred and α and β are constants. By assuming that acoustic emission is proportional to inelastic deformation, this relation can be compared to empirical creep laws. It is similar to the relation given by Lomnitz and fits the data more closely than other creep laws that were functions of time rather than number of acoustic emission events. The value of α was found to decrease systematically with increasing differential stress, and in one experiment became negative before sample failure.

Introduction

Inelastic deformation in rock, or creep, is commonly divided into three stages. When rock is placed under sufficient stress, it initially undergoes primary creep, a period in which the strain rate is inversely proportional to time. When the strain rate has dropped off sufficiently, a period of secondary creep begins, in which there is a small but constant strain rate. If the rock is held at constant stress for long enough, the strain rate will suddenly increase until failure occurs. This period is known as tertiary creep.

A number of investigators have found that microfracture activity caused by the opening of small cracks in rock is proportional to creep strain. Mogi (1962) found this to be true for creep experiments in bending. Hardy *et al.* (1969) reported the same results for samples in uniaxial compression. Scholz (1968a) reported a high correlation between inelastic volumetric strain and acoustic emission in uniaxial compression.

In the four experiments reported here, our primary intention was to study the locations of microfractures in rocks under stress. Because of the fast recording capabilities of our monitoring equipment, we were also able to study the acoustic emission rate during these experiments. We will discuss our findings on how microseismic activity is related to stress, creep strain, and creep strain rate.

Method

Cylindrical samples of Weber Sandstone and Westerly Granite 19.05 cm long and 7.62 cm in diameter were prepared. These unusually large samples were used to improve the relative accuracy of the locations of microfractures producing acoustic emission. Each sample was placed in a polyurethane sleeve to isolate it from con-

fining fluid during the experiments. Six piezoelectric transducers with resonant frequency of 600 kHz were cemented to each sample with epoxy to monitor acoustic emission from the rock. After being mounted in a pressure vessel, the samples were held at a constant 1,000 bars confining pressure throughout each experiment by means of a servo-controlled hydraulic pump. As shown in Figure 1, an additional axial load could be applied by advancing a piston against the end of the sample.

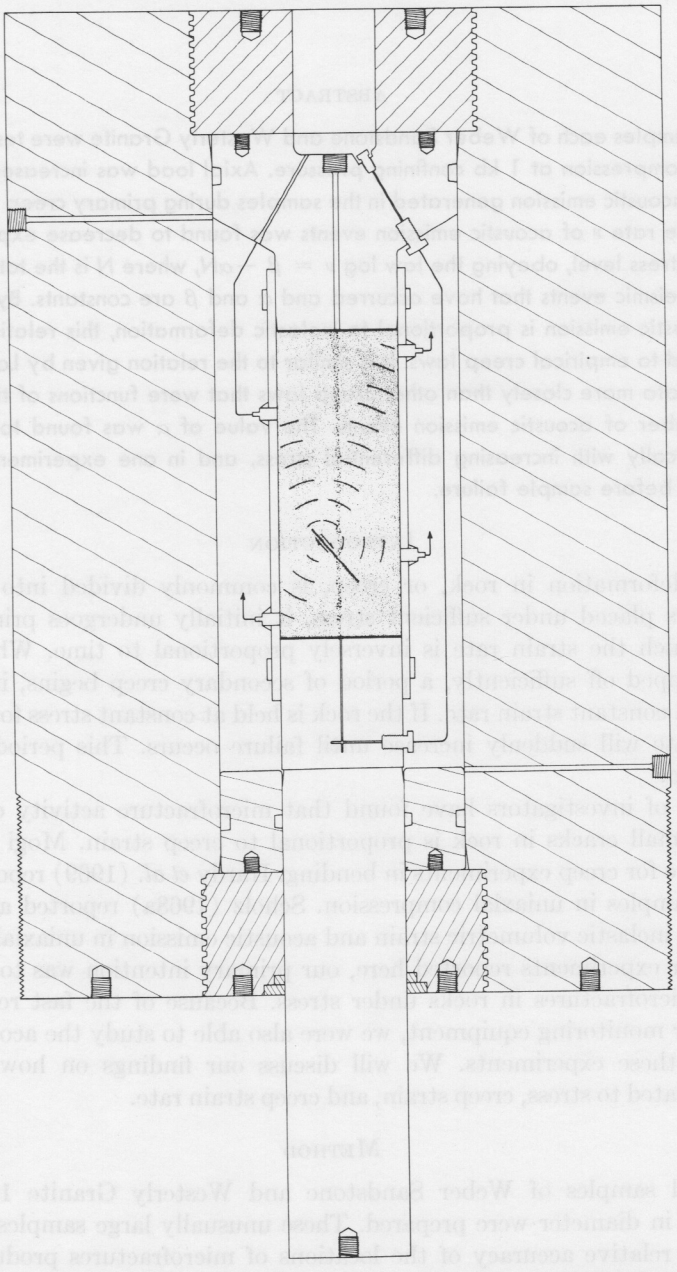

FIG. 1. Schematic diagram of the loading system. The sample shown shaded is contained within a pressure vessel. Load is applied to sample by means of a piston which moves through an O-ring seal. Acoustic emission generated by microfractures in the rock is monitored by transducers attached to the sample.

The procedure in each experiment was to raise the differential stress to a predetermined level and then hold it constant by means of a servo-controlled hydraulic ram. The acoustic emission generated by the loading of the sample was monitored for at least 15 min. The load was then increased and held constant at a new level while the acoustic emission was recorded. In this way differential stress was increased in steps until macroscopic failure occurred. Failure was so violent in three of the experiments that it dislodged one or more of the transducers attached to the sample. As a result, in only one of the four experiments could the post-failure acoustic emission be monitored.

The outputs of the six transducers attached to the samples were amplified and fed into an electronic timing system. In this system, each time a microfracture event occurs, such as slippage along a grain boundary, the acoustic waves that are produced travel to the six transducers mounted on the sample. When the station closest to the event registers an above-threshold signal corresponding to the arrival of the acoustic wave, timers are started on the other five channels. As each channel registers the wave's arrival, the state of its clock is recorded to within 0.1 μsec accuracy. These relative arrival times are automatically digitized and recorded on magnetic tape for later computer analysis. A burst of up to 32 events can be recorded in about 2 msec for a short-term repetition rate of over 16,000 per sec. The long-term repetition rate is limited by the transfer time from buffer memory to tape and is about 300 per second, or about 18,000 acoustic emission events per minute. A computer program calculates the location of each microseismic event from the acoustic emission data using an iterative technique employed by seismologists in locating earthquake hypocenters. For a more detailed description of this process and an analysis of the locations of the acoustic emission events monitored in these four experiments, refer to Byerlee and Lockner (1975) and Lockner and Byerlee (1975).

On each of the six input channels, a minimum amplitude signal is required to activate the timing mechanism. The threshold levels of all of the channels are balanced before each experiment; however, this threshold level was different for each of the four experiments. Because of this, there was a large variation in the number of events recorded in each experiment.

Results

Figures 2 to 5 show the stress history and frequency of microfracture events monitored during the four experiments. In experiment I, a sample of Weber Sandstone was held at 4 kb differential stress for 7 days (Figure 2). After one day, a system malfunction momentarily dropped the confining pressure 250 bars. This was accompanied by a rapid rise in the acoustic emission which then monotonically decreased for the remainder of the 7 days. At this point, differential stress was raised to 4.5 kb and held constant until failure. When the stress was increased, the acoustic emission rate rose to over 10^5 events per hour, decreased to $10^{4.5}$ events per hour, then increased until failure. Approximately 15 min before failure, the acoustic emission rate had increased beyond the recording limit of our equipment. To correct this, we decreased the amplification of the transducer signals by a factor of two. At failure, differential stress dropped to 3.26 kb. Acoustic emission was recorded for 15 min more, after which the experiment was ended.

In experiment II (Figure 3), differential stress was raised in six steps until failure occurred at 5.7 kb. Weber Sandstone was used in this experiment. In experiments III and IV (Figures 4 and 5), samples of Westerly Granite were used. Here, failure occurred at 9.25 and 9 kb differential stress, respectively.

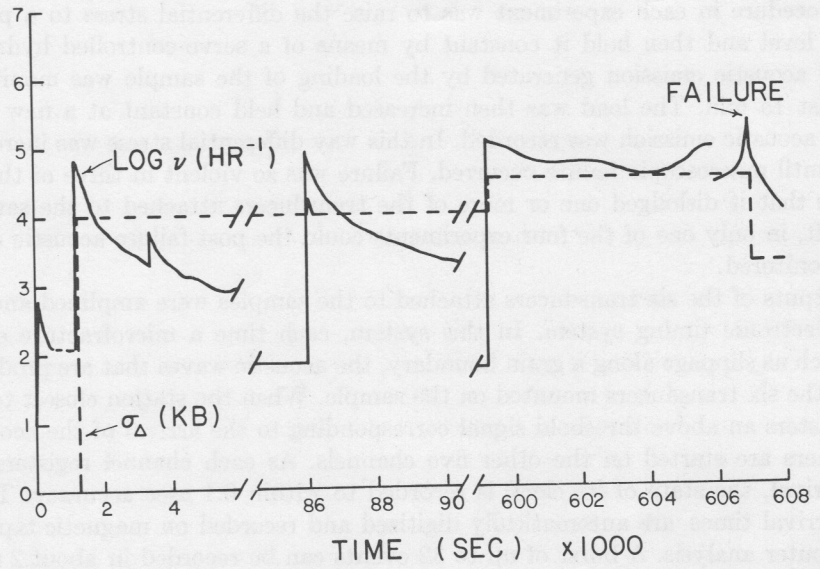

FIG. 2. Stress history and accompanying acoustic emission for experiment I, using Weber Sandstone. At 86,000 sec, the confining pressure dropped momentarily causing an abrupt increase in the acoustic emission rate. Failure occurred at 607,100 sec. At 606,000 sec, acoustic emission was occurring faster than the system could record it. The gain on the transducer signals was then lowered to reduce the number of signals that triggered the system.

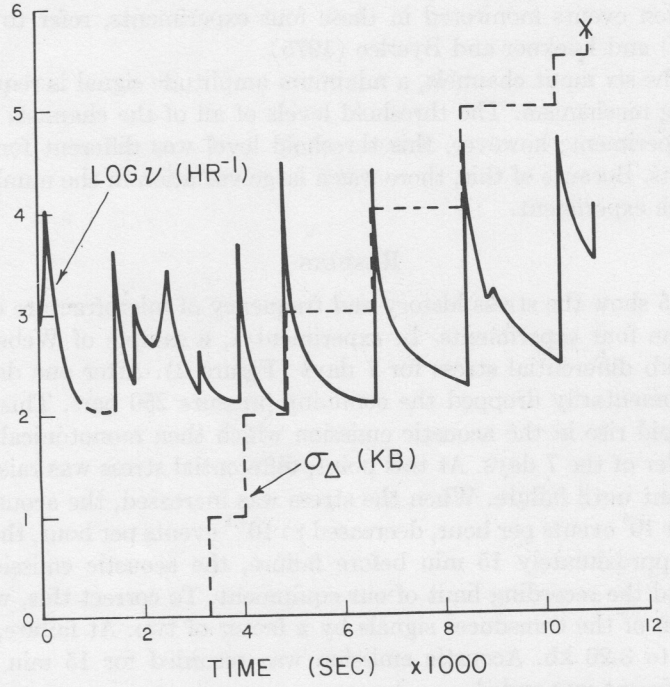

FIG. 3. Stress history and accompanying acoustic emission for experiment II, using Weber Sandstone. Acoustic emission at zero differential stress was caused by opening and closing of cracks as confining pressure was repeatedly raised and lowered before the start of the creep experiment.

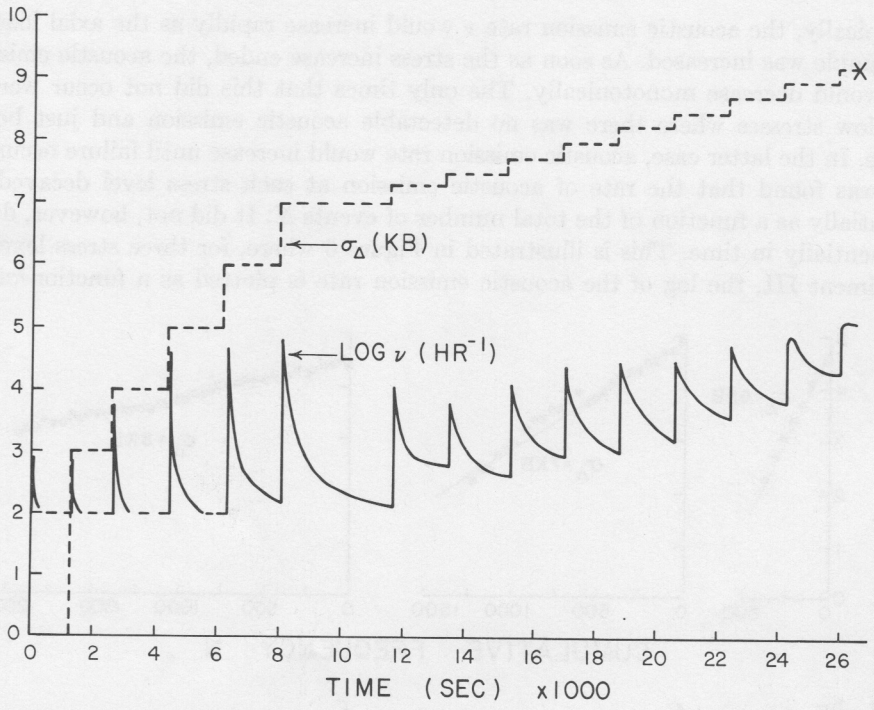

FIG. 4. Stress history and accompanying acoustic emission for experiment III, using Westerly Granite. Sample failed at 9.25 kb differential stress.

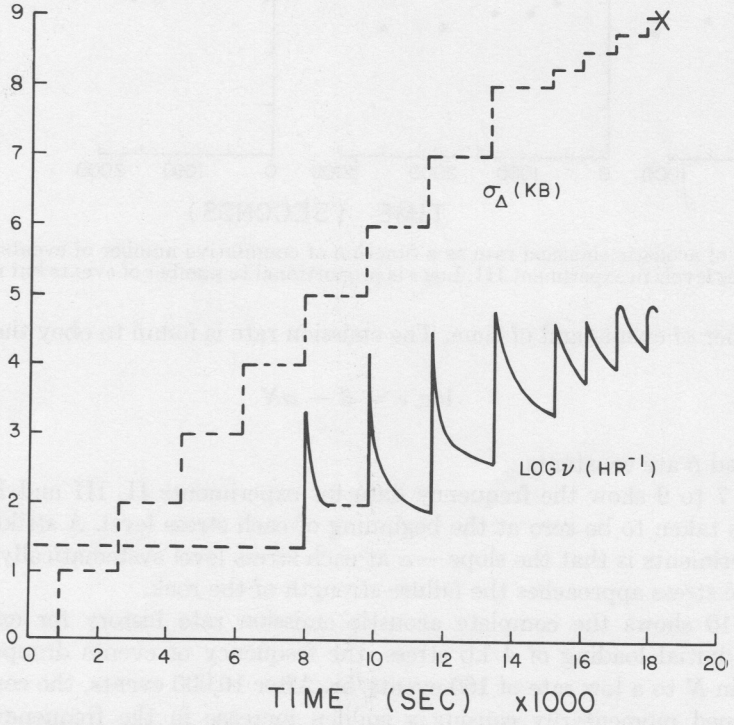

FIG. 5. Stress history and accompanying acoustic emission for experiment IV, using Westerly Granite. Sample failed at 9 kb differential stress.

Typically, the acoustic emission rate ν would increase rapidly as the axial load on the sample was increased. As soon as the stress increase ended, the acoustic emission rate would decrease monotonically. The only times that this did not occur were at very low stresses where there was no detectable acoustic emission and just before failure. In the latter case, acoustic emission rate would increase until failure occurred.

It was found that the rate of acoustic emission at each stress level decayed exponentially as a function of the total number of events N. It did not, however, decay exponentially in time. This is illustrated in Figure 6 where, for three stress levels in experiment III, the log of the acoustic emission rate is plotted as a function of the

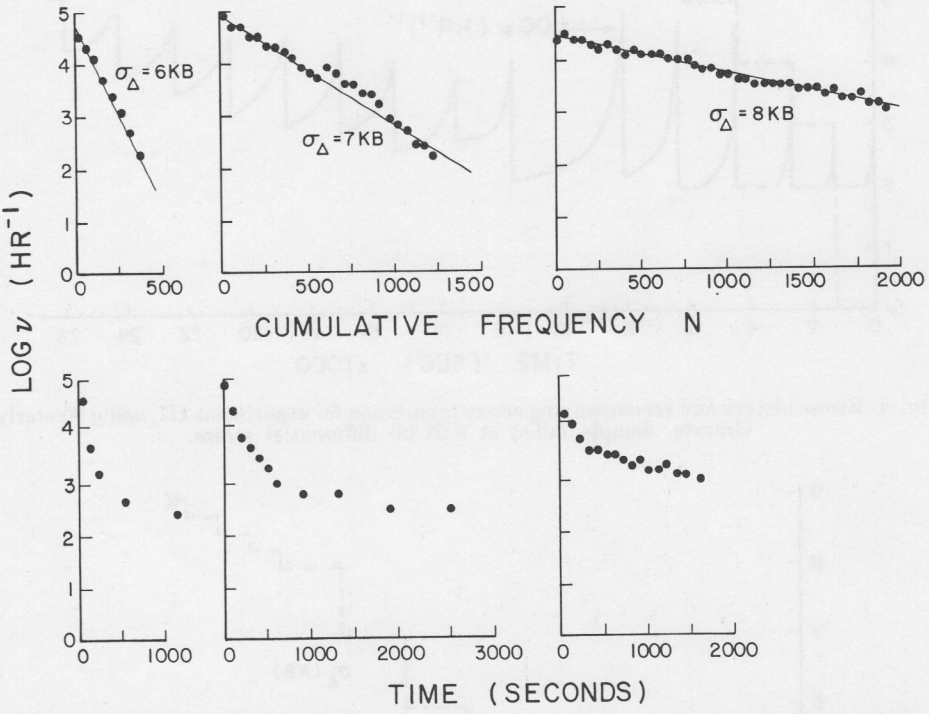

FIG. 6. Log of acoustic emission rate as a function of cumulative number of events and time for three stress levels in experiment III. Log ν is proportional to number of events but not to time.

total number of events and of time. The emission rate is found to obey the law

$$\log \nu = \beta - \alpha N \tag{1}$$

where α and β are constants.

Figures 7 to 9 show the frequency data for experiments II, III and IV. In these plots, N is taken to be zero at the beginning of each stress level. A striking result of these experiments is that the slope $-\alpha$ at each stress level systematically approaches zero as the stress approaches the failure strength of the rock.

Figure 10 shows the complete acoustic emission rate history for experiment I. After the initial loading of 4 kb stress, the frequency of events dropped off exponentially in N to a low rate of 160 events/hr. After 16,000 events, the confining pressure dropped momentarily causing a sudden increase in the frequency of events. Upon readjusting the confining pressure at 17,500 events, the frequency again dropped

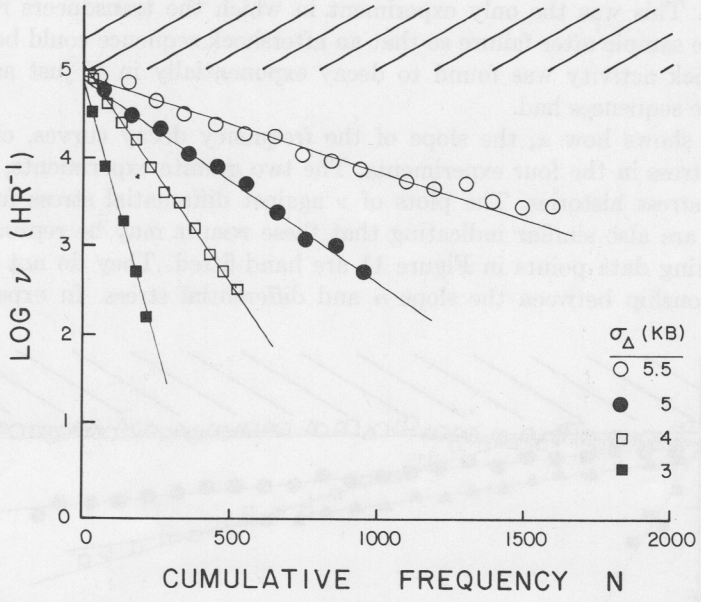

FIG. 7. Log of acoustic emission rate as a function of cumulative number of events for stress levels in experiment II. Hatched region is the upper limit of the recording system.

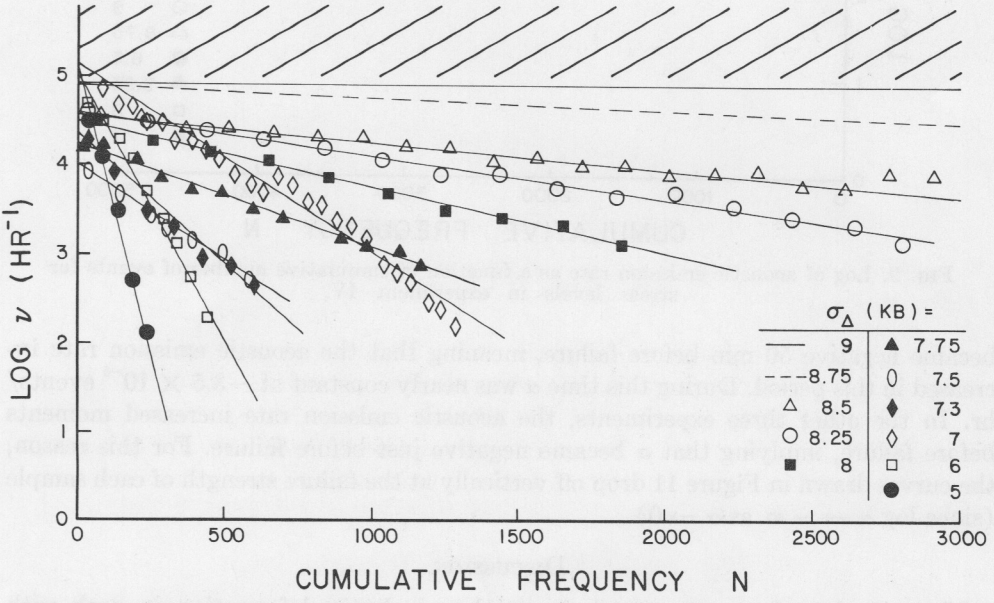

FIG. 8. Log of acoustic emission rate as a function of cumulative number of events for stress levels in experiment III.

exponentially in N to a rate of about 150 events/hr. After 45,000 events (7 days) differential stress was raised to 4.5 kb, the acoustic emission rate immediately rose to the recording limit of our equipment, over 10^5 events/hr. It then gradually decreased, leveled off, and finally increased until failure. The axial strain rate of the sample behaved in a similar fashion of first decreasing, going to zero, and then increasing

until failure. This was the only experiment in which the transducers remained attached to the sample after failure so that an aftershock sequence could be monitored. The aftershock activity was found to decay exponentially in N just as the earlier microfracture sequences had.

Figure 11 shows how α, the slope of the frequency decay curves, changes with differential stress in the four experiments. The two granite experiments, III and IV, had similar stress histories. The plots of ν against differential stress for these two experiments are also similar indicating that these results may be reproducible. The lines connecting data points in Figure 11 are hand-fitted. They do not suggest any simple relationship between the slope α and differential stress. In experiment I, α

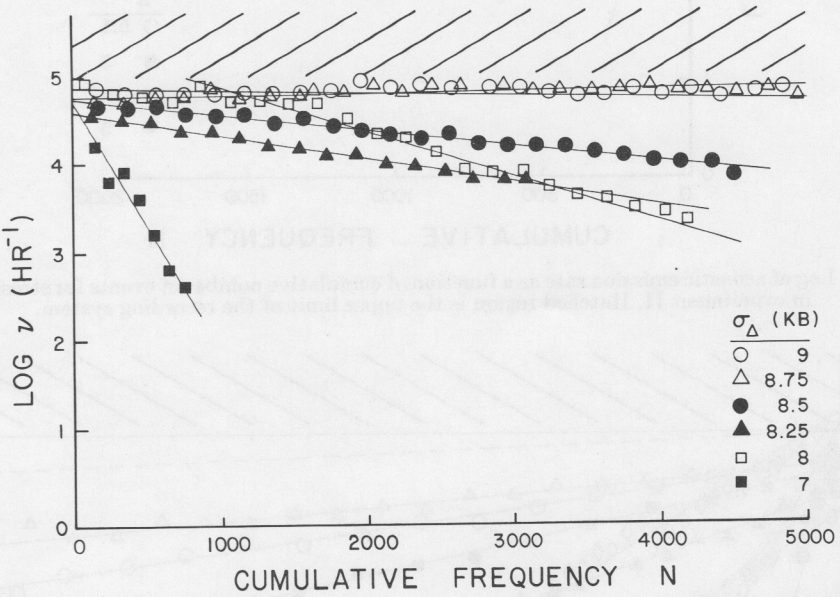

FIG. 9. Log of acoustic emission rate as a function of cumulative number of events for stress levels in experiment IV.

became negative 50 min before failure, meaning that the acoustic emission rate increased in this period. During this time α was nearly constant at -3.5×10^{-5} events/hr. In the other three experiments, the acoustic emission rate increased moments before failure, implying that α became negative just before failure. For this reason, the curves drawn in Figure 11 drop off vertically at the failure strength of each sample (since $\log \alpha \to -\infty$ as $\alpha \to 0$).

DISCUSSION

Many workers have attempted to correlate inelastic deformation in rock with microseismic activity. Scholz (1968b) proposed that creep in brittle rock at low temperature is due to time-dependent cracking. By assuming a Markov process for relating cracking to the stress field, he derived a transient creep law in which the volumetric strain Δ is given by

$$\Delta = c_1 \log t. \tag{2}$$

Here c_1 is a constant. Hardy *et al.* (1969) conducted incremental creep tests on un-

confined samples of limestone, sandstone, and granite. They found that cumulative microseismic activity N was proportional to strain.

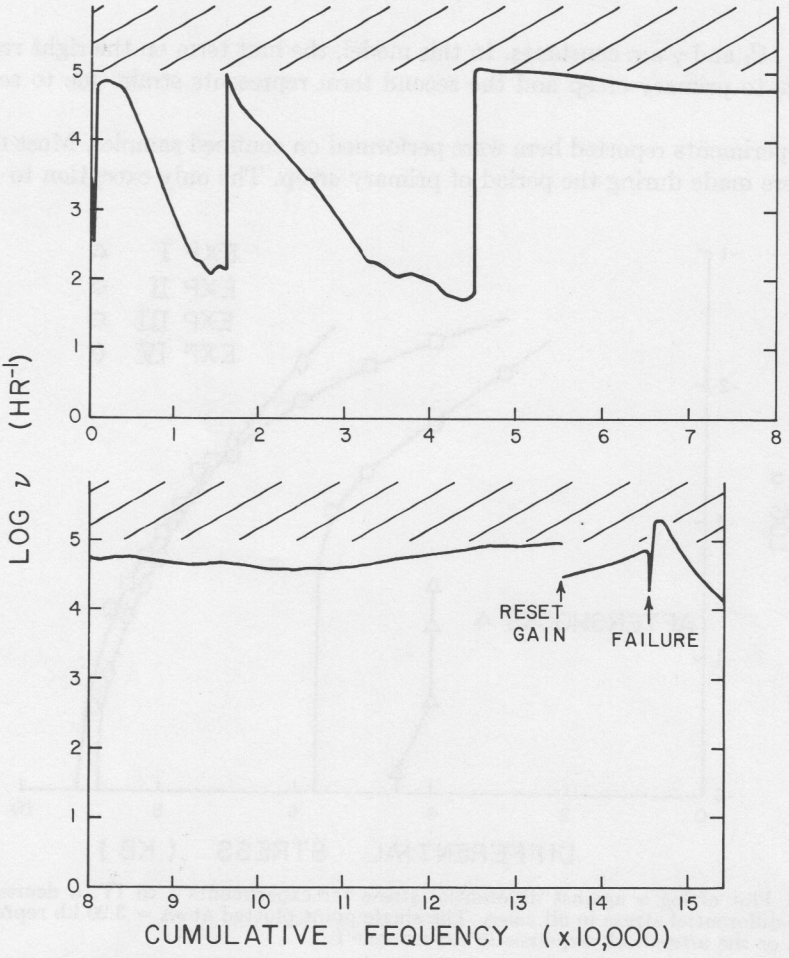

FIG. 10. Log of acoustic emission rate as a function of cumulative number of events for experiment I. Failure occurred at $N = 146{,}000$ events.

A number of empirical formulas have been proposed to describe transient inelastic deformation. The following are taken from Kennedy (1962) and are typical of empirical creep laws

$$\epsilon = a + b \log t \qquad \text{(Phillips)} \qquad (3)$$

$$\epsilon = a \{\log [1 + bt]\}^{2/3} \qquad \text{(Mott and Nabarro)} \qquad (4)$$

$$\epsilon = a \log t + bt + c \qquad \text{(Weaver)} \qquad (5)$$

$$\epsilon = a + bt^n \qquad \text{(Swift and Tyndall)} \qquad (6)$$

$$\epsilon = a \log t + bt^n + ct \qquad \text{(Wyatt)} \qquad (7)$$

Hardy *et al.* (1969) fit their data to the generalized Burgers model given by

$$\epsilon = C_2(1 - e^{-\gamma t}) + C_3 t \tag{8}$$

where C_2, C_3 and γ are constants. In this model, the first term on the right represents strain due to primary creep and the second term represents strain due to secondary creep.

The experiments reported here were performed on confined samples. Most measurements were made during the period of primary creep. The only exception to this was

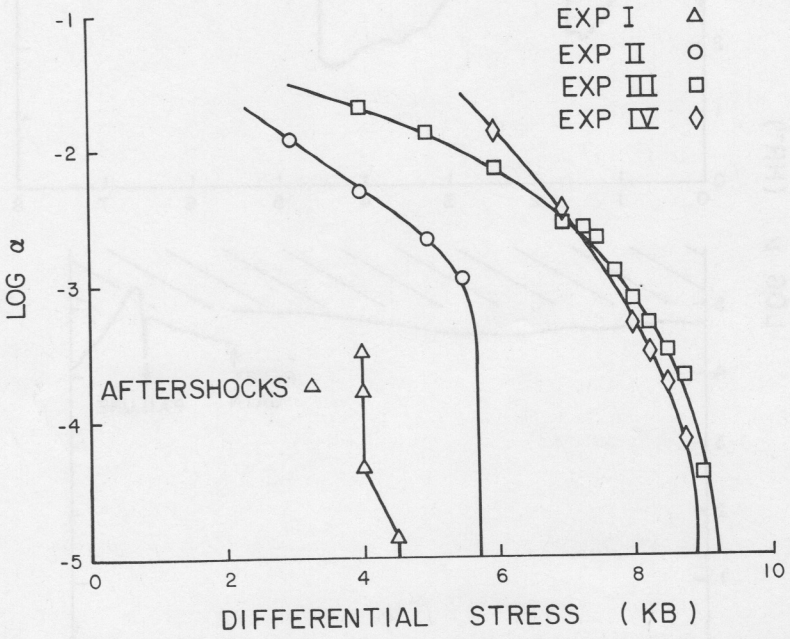

FIG. 11. Plot of log α against differential stress for experiments I to IV. α decreased with increasing differential stress in all cases. The single point plotted at $\sigma\Delta = 3.26$ kb represents the value of α or the aftershock sequence in experiment I.

experiment I in which acoustic emission was recorded during all three stages of creep.

These results indicate that during primary creep, acoustic emission frequency decays exponentially in N. This relation can be rewritten as a function of time giving

$$N = (1/\alpha) \log [1 + 2.3\ (10^{\beta})\alpha t] \tag{9}$$

or

$$\nu = dN/dt = 1/(2.3\alpha t + 10^{-\beta})\ . \tag{10}$$

Assuming, as Hardy *et al.* (1969) showed, that cumulative microseismic activity N is proportional to strain, equation (9) can be compared to the empirical strain relation by multiplication by a constant. If this is done, none of equations (3) to (8) will adequately fit all the data. Equation (4) would be equivalent to equation (9) if the $\frac{2}{3}$ power were replaced by unity. For $\alpha t \gg 10^{-\beta}$, equations (3) and (9) are the

same. Indeed, at high differential stresses, equation (3) fits the data well for $t > 5$ min.

Lomnitz (1956) performed creep tests on rock samples subjected to torsional loading at low stress. He reported that under these conditions time-dependent strain obeyed the law

$$\epsilon(t) = q \ln (1 + at) \tag{11}$$

where q and a are constants. Equations (9) and (11) are of the same form, suggesting that the relation Lomnitz found for primary creep at low stress may be applicable over a broad range of stresses. Lomnitz reported a to be of the order of 10^3 sec^{-1} whereas in our experiments, a varies from 1 to 0.001 sec^{-1}.

The function given by equation (1) is well defined for all positive N and for all positive and negative α and β. When expressed in the time domain as in equation (9), this is no longer the case. Here, for $\alpha \geqq 0$, ν is again well defined for all positive t. However, for $\alpha < 0$, there is a singularity at

$$t = -(1/\alpha)[10^{-(\beta+0.36)}]. \tag{12}$$

At this point, the acoustic emission rate would go to infinity. In a real sample, the cracking that occurs during failure would not be well represented by equation (9), which is derived from acoustic emission during primary creep. However, it is interesting to note that in all four experiments, as the failure strength was approached, α systematically decreased and, in the case of experiment I, became negative before failure. For negative α, the time when the acoustic emission rate "blows up" could be thought of as an upper limit on the time of failure since the density of cracks in the sample should eventually become large enough that they coalesce and lead to macroscopic failure. This would happen, of course, some time before N could go to infinity.

An interesting result in experiment I is the abrupt change in slope in the acoustic emission rate at low frequencies ($\log \nu < 2.3$). One explanation of this abrupt slope change is that it marks the transition from primary to secondary creep. If these two types of creep were the result of different processes, they could produce different acoustic emission rates. If both processes were occurring throughout each creep test, experiment I suggests that the primary creep acoustic emission initially masks the low level emission produced by the secondary creep process. However, if the experiment is continued long enough, the emission rate due to primary creep eventually dies off below that of the secondary creep. When this happens, the secondary creep rate becomes dominant. Owing to the nature of the log function, the transition from one creep rate to the other should be smooth, but over a short interval of N. This transition is masked by the scatter in the data in Figure 10. Secondary creep is generally characterized as a period of constant strain rate. If this were true, secondary creep would produce a constant acoustic emission rate. However, if the acoustic emission rate for $33{,}000 < N < 44{,}000$ events in Figure 10 is due to secondary creep, it indicates that the creep rate was decreasing at this time.

The fact that acoustic emission rate at constant stress obeys equation (1) has not been reported before. None of the commonly used empirical creep laws adequately fit the data. Presumably, there is an underlying physical process responsible for this simple relation. However, it is not clear from our experiments what this process might be. The fact that α goes to zero and then becomes negative before failure is simply

restating the fact that under proper conditions, rocks display secondary and tertiary creep before failure. However, as seen in Figure 11, the change in α could be of use in recognizing when a rock is approaching its failure strength. This could be of great value in predicting rock bursts in mines as well as in predicting earthquakes.

References

Byerlee, J. D. and D. Lockner (1975). Acoustic emission during fluid injection into rock in *Trans. Conference on Acoustic Emission in Geologic Structures and Materials* (in press), Pennsylvania State Univ.

Hardy, H. R., R. Y. Kim, R. Stefanko, and Y. J. Wang (1969). Creep and microseismic activity in geologic materials, paper presented at Eleventh Symposium on Rock Mechanics, University of California, Berkeley, 45 pp.

Kennedy, A. J. (1962). *Processes of Creep and Fatigue in Metals*. Oliver and Boyd, Edinburgh and London, 480 pp.

Lockner, D. and J. D. Byerlee (1975). Acoustic emission and fault formation on rocks, *Trans. Conference on Acoustic Emission in Geologic Structures and Materials* (in press), Pennsylvania State Univ.

Lomnitz, C. (1956). Creep measurements in igenous rocks, *J. Geology* **64**, 473–479.

Mogi, K. (1962). Study of the elastic shocks caused by the fracture of a heterogeneous material and its relation to earthquake phenomena, *Bull. Earthquake Res. Inst., Tokyo Univ.* **40**, 125–173.

Scholz, C. H. (1968a). Microfracturing and the inelastic deformation of rock in compression, *J. Geophys. Res.* **73**, 1417.

Scholz, C. H. (1968b). Mechanism of creep in brittle rock, *J. Geophys. Res.* **73**, 3295–3302.

U.S. Geological Survey
345 Middlefield Road
Menlo Park, CA 94025

Manuscript received June 14, 1976